



NRC Publications Archive Archives des publications du CNRC

X-ray diffraction analysis of nanoparticles: recent developments, potential problems and some solutions

Whitfield, Pamela; Mitchell, Lyndon

This publication could be one of several versions: author's original, accepted manuscript or the publisher's version. /
La version de cette publication peut être l'une des suivantes : la version prépublication de l'auteur, la version
acceptée du manuscrit ou la version de l'éditeur.

Publisher's version / Version de l'éditeur:

International Journal of Nanoscience, 3, 6, 2004

NRC Publications Record / Notice d'Archives des publications de CNRC:

<https://nrc-publications.canada.ca/eng/view/object/?id=9973d6d6-7de3-47ab-bed9-a72a649cdab6>

<https://publications-cnrc.canada.ca/fra/voir/objet/?id=9973d6d6-7de3-47ab-bed9-a72a649cdab6>

Access and use of this website and the material on it are subject to the Terms and Conditions set forth at

<https://nrc-publications.canada.ca/eng/copyright>

READ THESE TERMS AND CONDITIONS CAREFULLY BEFORE USING THIS WEBSITE.

L'accès à ce site Web et l'utilisation de son contenu sont assujettis aux conditions présentées dans le site

<https://publications-cnrc.canada.ca/fra/droits>

LISEZ CES CONDITIONS ATTENTIVEMENT AVANT D'UTILISER CE SITE WEB.

Questions? Contact the NRC Publications Archive team at

PublicationsArchive-ArchivesPublications@nrc-cnrc.gc.ca. If you wish to email the authors directly, please see the first page of the publication for their contact information.

Vous avez des questions? Nous pouvons vous aider. Pour communiquer directement avec un auteur, consultez la première page de la revue dans laquelle son article a été publié afin de trouver ses coordonnées. Si vous n'arrivez pas à les repérer, communiquez avec nous à PublicationsArchive-ArchivesPublications@nrc-cnrc.gc.ca.



X-RAY DIFFRACTION ANALYSIS OF NANOPARTICLES: RECENT DEVELOPMENTS, POTENTIAL PROBLEMS AND SOME SOLUTIONS

PAMELA WHITFIELD

*Institute for Chemical Process and Environmental Technology
National Research Council Canada, 1200 Montreal Road
Ottawa, Ontario K1A 0R6, Canada*

LYNDON MITCHELL

*Institute for Research in Construction
National Research Council Canada, 1200 Montreal Road
Ottawa, Ontario K1A 0R6, Canada*

Powder X-ray diffraction has become a cornerstone technique for deriving crystallite size in nanoscience due to speed and “simplicity”. Unfortunately, this apparently simple technique commonly has unexpected problems. Anisotropic peak broadening related to crystallite shape, defects, and microstrain occurs frequently in nanomaterials and can significantly complicate the analysis. In some instances, the usage of the conventional single peak approach would give erroneous results, and in others, this type of analysis is not even possible. A number of different nanocrystalline oxides have been examined to determine their crystallite sizes by different techniques. They differ in terms of crystal symmetry, crystallinity, density, and present different challenges with regard to size analysis.

Keywords: X-ray diffraction; oxides.

1. Introduction

Powder diffraction techniques have a wide variety of applications in compositional, structural, microstructural and many other areas. The ease in data collection makes its application to the microstructure of nanomaterials an obvious choice. In the study of nanomaterials, the crystallite size is usually the sole factor of interest. The broadening of reflections in a powder diffraction pattern contains much information, such as crystallite strain, shape and stacking faults, which are often not considered. Nanomaterials even have their own unique problems, such as multiply twinned particle phenomena in metal nanoparticles. The extensive peak broadening and possible overlap exhibited by nanomaterials can even make determining phase purity a nontrivial process, and mis-identification of a two-phase system as being single-phase could lead to some very misleading results. Visual inspection is often insufficient where closely related phases can co-exist, e.g., in solid solution series.

Full-pattern profile fitting techniques such as Rietveld analysis can assist greatly in gauging sample purity.

The first description of size broadening was given by Scherrer in 1918,¹ although the first rigorous theory of line broadening was formulated in 1944.² Williamson–Hall size-strain analysis³ was developed in 1953 as a method to separate size and strain effects by their angular dependence. Since then, most studies have been carried out using either Fourier peak shape-based Warren–Averbach,⁴ or simplified integral breadth methods. These methods give statistical measures of “column lengths”, L , usually volume-weighted (Fig. 1) rather than crystallite dimensions. Column lengths must be corrected to give real dimensions. Direct imaging techniques such as TEM provide number-weighted results (see Fig. 1). Conversion of column length to crystallite dimension(s) requires information on crystallite shape. While there is no anisotropic line broadening, it is relatively safe to assume a spherical shape, in which case:

$$\langle D \rangle_{\text{vol}} = \frac{4}{3} \langle L \rangle_{\text{vol}}, \quad (1)$$

where $\langle L \rangle_{\text{vol}}$ is the volume-weighted average column length, and $\langle D \rangle_{\text{vol}}$ is the volume-weighted average crystallite diameter.

Integral-breadth methods currently dominate routine size/strain analysis. These often assume that crystallite size broadening is Lorentzian and strain broadening Gaussian, referred to in this paper as the LG approach, although the choice is rather arbitrary and has been demonstrated to be unreliable. Recently, it has been shown that size and strain broadening are each more accurately modeled by Voigt functions.⁶ Size and strain contributions are still separated by the $1/\cos(\theta)$ and

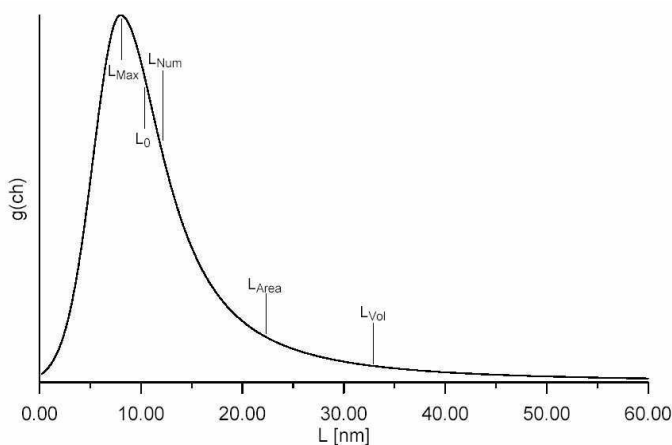


Fig. 1. Schematic representation of a column height distribution with the important statistical points indicated. L_{Max} = most probable value, L_0 = median value, L_{Num} = number-weighted mean, L_{Area} = area-weighted mean, and L_{Vol} = volume-weighted mean. Reproduced with permission from Topas 2.1 manual.⁵

$\tan(\theta)$ dependence of the individual functions. The double-Voigt approach performed well in a Round-Robin organized to compare size results from various techniques for analyzing powder diffraction data.⁷

A novel technique particularly suited to nanoparticulate materials is the use of Debye scattering analysis to yield radial distribution functions.⁸ In this context, crystallite diameters are assumed to be the maximum interaction distance on a next-nearest neighbor basis. For the purpose of determining crystallite size, conventional wide-angle X-ray techniques can be used satisfactorily,⁹ even with the truncation problems and limited range. This technique does not rely on any underlying order, so is suited to poorly crystalline and amorphous materials.

2. Experimental

A number of different nanocrystalline powders were analyzed for size characteristics using a number of different techniques. They were commercial CeO₂ (Nanoscale Materials Inc.) and laboratory synthesized LiMn₂O₄ and alumina materials. Ceria is used in Solid Oxide Fuel cells (SOFCs), and LiMn₂O₄ is an established cathode material for lithium batteries. The spinel and alumina were produced using a variation on the sucrose method for producing nanocrystalline oxides.¹⁰

Diffraction data for this paper were collected from a parallel-beam CuK α Bruker D8, and a Scintag XDS2000 CuK α Bragg–Brentano diffractometer. Instrument and emission source profiles were modeled using NIST LaB₆ 660 and 660a profile standards.

The software used to analyze the data using the “double-Voigt” approach was a beta version of Bruker’s Topas 2.1 software.⁵ Fourier radial distribution function analysis was carried out using the program RAD.¹¹ Selected samples were also examined using a Hitachi S4800 FEG-SEM.

3. Results and Discussion

The diffraction data for all the samples are shown in Fig. 2. The alumina shows very poor crystallinity, and it is not possible to identify its polymorph. Ceria is frequently used as a standard material for the study of nanomaterials and is expected to show isotropic broadening behavior. Structural refinements using both the LG and double-Voigt approaches were carried out. The double-Voigt fitting achieved a better fit to the data than the LG approach as seen in Fig. 3, with an R_{wp} of 7.1% as opposed to 7.8% for the LG approach. In general terms, the smaller the value of R_{wp} ,¹² the better the fit, although noise and high backgrounds can impact R_{wp} values. Assuming a spherical shape, a crystallite diameter $\langle D \rangle_{\text{vol}}$ of 8.0(1) nm was derived. This value compares favorably with the manufacturers’ claim of ≤ 7 nm.

The Williamson–Hall plot for data collected from the LiMn₂O₄ spinel are shown in Fig. 4. In Williamson–Hall plots, $\langle L \rangle_{\text{vol}}$ is extracted from the intercept, and strain from the slope in a semi-quantitative manner. It is apparent from the plot that there are some hkl -dependent differences in the apparent size and strain, i.e., the

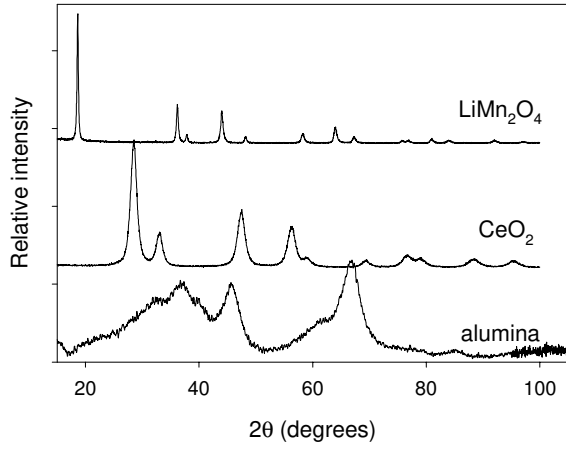
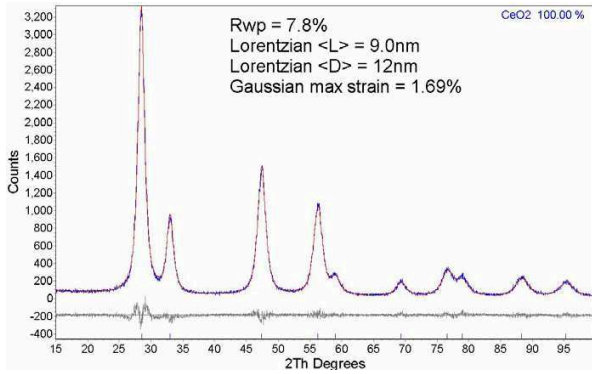
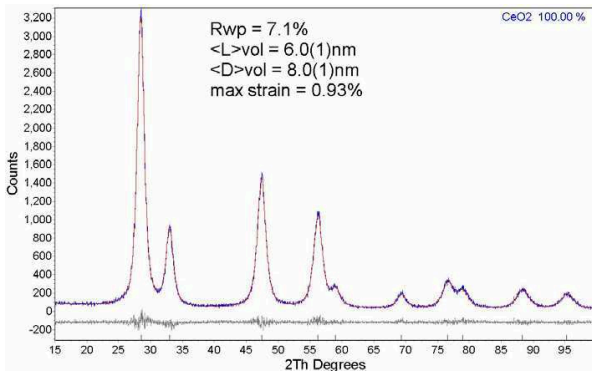


Fig. 2. X-ray diffraction patterns of the various samples. The intensities have been rescaled to afford better comparison of the weaker patterns.



(a)



(b)

Fig. 3. Difference plot yielded by (a) LG and (b) double-Voigt Rietveld refinement of the ceria structure.

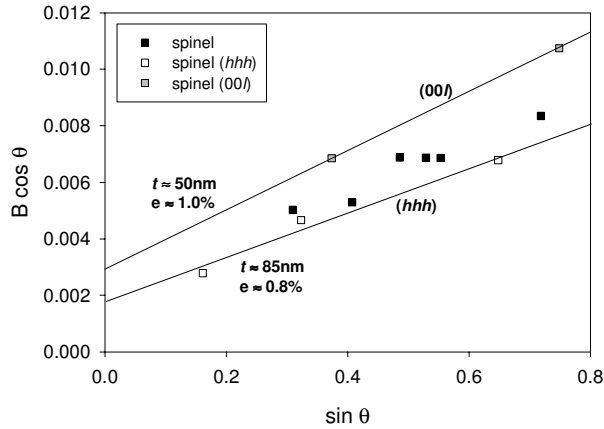


Fig. 4. Williamson–Hall plot for the LiMn_2O_4 . The (hhh) and $(00l)$ reflections are plotted separately. B was extracted from FWHM values of Pearson VII fitting to the sample and the LaB_6 standard.

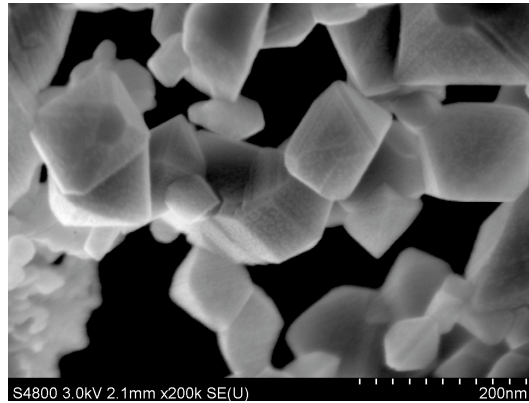


Fig. 5. Micrograph of the nanocrystalline LiMn_2O_4 material.

apparent size for the $00l$ reflections is smaller than those for the (hhh) reflections), e.g., the (222) . This suggests that the spinel crystallites have a distinct shape. Cubic materials usually form crystal shapes somewhere in a continuum between a cube and an octahedron. The mathematical description of shape-dependent hkl broadening is complex in many instances, although papers describing the hkl -dependence in terms of apparent size for a number of simple shapes do appear in the literature.¹³ Fortunately, cubic materials form simple shapes, and $\langle 111 \rangle$ faceting of an octahedral crystallite would be expected to give rise to a larger apparent size in the $[111]$ direction than the $[001]$. Therefore, the diffraction data suggests that the crystallites are octahedral in shape, with apparent dimensions of approximately 85 nm in the $[111]$ direction. Such a conclusion is consistent with the observations of the sample by FEG-SEM as seen in Fig. 5.

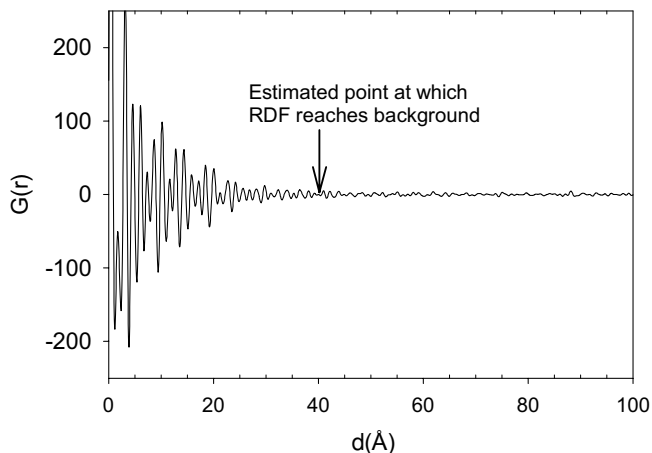


Fig. 6. Reduced radial distribution function calculated from the diffraction data of the nanocrystalline alumina.

The alumina could not be analyzed using conventional techniques, so a Debye scattering-based radial distribution function was calculated for this phase. Trials with other nanocrystalline samples indicated that comparable values are obtained to other diffraction methods. Size is indicated by the point at which $G(r)$, or electron density, reaches zero. The Fourier transform introduces background noise, introducing an error in the point at which the function reaches zero. The graph in Fig. 6 indicates a crystallite size of approximately 40 Å or 4 nm. This technique does not produce column lengths and is a direct measure of crystallite dimension.

4. Conclusions

It has been shown that a variety of techniques can be employed to extract size and sometimes strain data from diffraction data. The choice of technique depends largely on many complicating factors. One may have to resort to exotic methods based on Debye scattering where crystallinity is poor and crystal symmetry is uncertain. Crystallite shape effects must also be considered, even in cubic materials. Williamson–Hall plots can be useful in determining hkl -dependent broadening, and even suggest shapes for crystallites. The double-Voigt model for peak size/strain broadening can be employed successfully in full-pattern peak fitting methods.

Acknowledgments

The authors would like to thank Dr. Isobel Davidson, Dr. Arnt Kern and Dr. Alan Coelho for discussions on this paper. Mr. Tai Sato is thanked for allowing the authors to use his alumina sample for this paper. Mr. Yves Giroux of Hitachi Electron Microscope Division is thanked for permission to use the image in Fig. 5.

References

1. P. Scherrer, *Nachrichten von der Gesellschaft der Wissenschaften zu Göttingen* (1918), pp. 98–100.
2. A. R. Stokes and A. J. C. Wilson, *Proc. Phys. Soc.* **56**, 174 (1944).
3. G. K. Williamson and W. H. Hall, *Acta Metallurgica* **1**, 22 (1953).
4. B. E. Warren and B. L. Averbach, *J. Appl. Phys.* **21**, 595 (1950).
5. Bruker AXS. TOPAS V2.1 user manual, Karlsruhe, Germany, 2003.
6. D. Balzar and H. Ledbetter, *Advances in X-Ray Analysis* **38**, 397 (1995).
7. D. Balzar and N. C. Popa, Report on the size/strain round robin, *Commission of Powder Diffraction Newsletter*, No. 28, International Union of Crystallography (2002), pp. 14–15.
8. B. D. Hall, *J. Appl. Phys.* **87**, 1666 (2000).
9. B. D. Hall, D. Zanchet and D. Ugarte, *J. Appl. Crystallogr.* **33**, 1335 (2000).
10. L. D. Mitchell, P. S. Whitfield, J. Margeson and J. J. Beaudoin, *J. Mat. Sci. Lett.* **21**, 1773 (2002).
11. K. Petrov, *J. Appl. Crystallogr.* **22**, 387 (1989).
12. R. A. Young, *The Rietveld Method* (Oxford Science Publications, Oxford, 1995).
13. J. I. Langford and A. J. C. Wilson, *J. Appl. Crystallogr.* **11**, 102 (1978).